



**Enhanced Dielectric and Piezoelectric Properties of  
 $\text{Ba}_{0.8}\text{Sr}_{0.2}\text{Ti}_{1-x}\text{Sn}_x\text{O}_3$  for Energy Harvester Applications**

by

**Nur Nadia Nasika Binti Mahamad Nasir  
(2030313173)**

A thesis submitted in fulfillment of the requirements for the degree of  
Master of Science (Electronic Engineering)

**Faculty of Electronic Engineering Technology  
UNIVERSITI MALAYSIA PERLIS**

2021

## ACKNOWLEDGEMENT

I am thankful to Allah S.W.T because, with His blessings, I was able to complete this project successfully.

Special thanks to my supervisor, Associate Professor Ir. Ts. Dr. Rozana Aina Maulat Osman, thank you for the guidance, advice, encouragement, suggestions, and constructive views throughout my master's study. I am so grateful for the valuable knowledge she has given me. I was indeed lucky to have an excellent supervisor like her. Besides that, thank you to Professor Dr. Prabakaran A/L Poopalan being as co-supervisor and sharing interesting ideas for my master project. Not to forget, I also thank Associate Professor Ts. Dr. Mohd Sobri Idris for the knowledge and experience he has shared with me.

Furthermore, I would like to thank the technical staff and friends, especially Dr. Ku Noor Dhaniah Ku Muhsen, postdoctoral, for their motivational support and voluntary participation in completing all required information. Special thanks to the Dean of the School of Microelectronic Engineering, UniMAP, for allowing me to further my studies in the field of Master of Science (Electronics Engineering).

I would like to thank the Impedance Spectroscopy Laboratory director at the School of Applied Physics, Universiti Kebangsaan Malaysia, Associate Professor Dr. Mohamad Hafizuddin Hj Jumali, for allowing me to use the piezoelectric tester for piezoelectric constant measurement.

I acknowledge my sincere indebtedness and gratitude to my mom, Maznee binti Ibrahim, and my dad, Mahamad Nasir bin Abdullah for their love, dream, and sacrifice throughout my life. I am thankful for their sacrifice, patience, and understanding that was inevitable to make this work possible. I cannot find the appropriate words that could adequately describe my appreciation for their devotion, support, and faith in my ability to achieve my dreams. Finally, I would like to thank my siblings Muhaimin, Nabila, and Naja, for cheering my day and made me never give up inspiring them with the success I have achieved.

## TABLE OF CONTENTS

	<b>PAGE</b>
<b>DECLARATION OF THESIS</b>	<b>i</b>
<b>DECLARATION OF THESIS</b>	<b>i</b>
<b>ACKNOWLEDGEMENT</b>	<b>ii</b>
<b>TABLE OF CONTENTS</b>	<b>iii</b>
<b>LIST OF TABLES</b>	<b>vi</b>
<b>LIST OF FIGURES</b>	<b>viii</b>
<b>LIST OF ABBREVIATIONS</b>	<b>xii</b>
<b>LIST OF SYMBOLS</b>	<b>xiii</b>
<b>ABSTRAK</b>	<b>xiv</b>
<b>ABSTRACT</b>	<b>xv</b>
<b>CHAPTER 1 : INTRODUCTION</b>	<b>1</b>
1.1 Research Background	1
1.2 Mechanism of piezoelectric materials	2
1.3 Problem statement	4
1.4 Objectives	5
1.5 Scope of study	5
1.6 Thesis structure	6
<b>CHAPTER 2 : LITERATURE REVIEW</b>	<b>7</b>
2.1 Introduction	7
2.2 Piezoelectricity	7

2.3	Properties of piezoelectric for Energy Harvester Applications	11
2.3.1	Polarisation Directions and Mechanical Stress Axis Nomenclature	13
2.4	Dielectric Properties and Dissipation factor	14
2.5	Tolerance factor	15
2.6	Perovskite Structure	17
2.7	Materials for Piezoelectric	20
2.7.1	Lead Zirconate Titanate (PZT)	20
2.7.2	Barium Titanate ( $\text{BaTiO}_3$ )	22
2.7.3	Barium Strontium Titanate (BST)	25
2.7.4	Barium Titanate Stannate (BTS)	29
2.8	Sn doped Barium Strontium Titanate (BSTS)	32
2.9	Summary	34
<b>CHAPTER 3 : METHODOLOGY</b>		<b>36</b>
3.1	Introduction	36
3.2	Sample preparation	36
3.3	Characterisations of the samples	39
3.3.1	X-Ray Diffraction Analysis	39
3.3.2	Impedance Spectroscopy Analysis	41
3.3.3	Scanning Electron Microscopy (SEM)	42
3.3.4	Piezoelectric Test Analysis	43
<b>CHAPTER 4 : RESULTS &amp; DISCUSSION</b>		<b>45</b>
4.1	Introduction	45
4.2	Structural analysis	45
4.2.1	Undoped sample ( $\text{Ba}_{0.8}\text{Sr}_{0.2}\text{TiO}_3$ )	45
4.2.2	Structural analysis of $\text{Ba}_{0.8}\text{Sr}_{0.2}\text{Ti}_{1-x}\text{Sn}_x\text{O}_3$ ( $0 \leq x \leq 0.10$ )	47
4.3	Electrical properties analysis	52

4.3.1	Undoped sample ( $\text{Ba}_{0.8}\text{Sr}_{0.2}\text{TiO}_3$ )	52
4.3.2	Impedance Spectroscopy Analysis for $\text{Ba}_{0.8}\text{Sr}_{0.2}\text{Ti}_{1-x}\text{Sn}_x\text{O}_3$ ( $0 \leq x \leq 0.10$ ) ceramics sintered at 1400 °C	57
4.4	Scanning Electron Microscopy (SEM) Analysis sintered at 1400 °C	69
4.5	Piezoelectric Analysis	71
4.5.1	The effect of electrical properties of $\text{Ba}_{0.8}\text{Sr}_{0.2}\text{Ti}_{1-x}\text{Sn}_x\text{O}_3$ ( $0 \leq x \leq 0.10$ ) at different sintering temperature.	73
4.5.2	Impedance spectroscopy analysis	73
4.5.3	Scanning Electron Microscopy (SEM) Analysis sintered at 1450 °C	78
4.5.4	Piezoelectric analysis	82
<b>CHAPTER 5 : CONCLUSION</b>		<b>85</b>
5.1	Conclusion	85
5.2	Recommendation for future work	87
<b>REFERENCES</b>		<b>89</b>
<b>LIST OF PUBLICATIONS</b>		<b>97</b>

## LIST OF TABLES

		PAGE
Table 2.1	List of commercial material with dielectric constant, piezoelectric constant, piezoelectric voltage constant, Curie temperature and applications	9
Table 2.2	Capacitance values for ceramic materials and their responsible phenomena (Sinclair, 1995)	15
Table 2.3	Tolerance factor value with their respective crystal structure (Buttner & Maslen, 1992)	16
Table 2.4	Piezoelectric coefficient, $d_{33}$ of BaTiO <sub>3</sub> comparison.	24
Table 2.5	The comparison of Sr doped BaTiO <sub>3</sub> as piezoelectric material	28
Table 2.6	The comparison of Sn doped BaTiO <sub>3</sub> as piezoelectric material	31
Table 2.7	The summary of piezoelectric material from the past study	35
Table 3.1	The drying temperature and drying duration of raw materials	37
Table 4.1	Crystal structure, space group, lattice parameter, and unit cell volume of Ba <sub>0.8</sub> Sr <sub>0.2</sub> Ti <sub>1-x</sub> Sn <sub>x</sub> O <sub>3</sub> ( $0 \leq x \leq 0.10$ )	50
Table 4.2	The Curie Weiss law, dielectric properties ( $T_c$ , $\epsilon_m$ , and $\epsilon_r$ ) tolerance factor ( $t$ ), and diffusiveness coefficient ( $\gamma$ )	61
Table 4.3	The conduction mechanism with their associated activation energy $E_{ACT}$ (eV) summarised by Ramond (Raymond et al., 2005)	68
Table 4.4	The piezoelectric characteristics of Ba <sub>0.8</sub> Sr <sub>0.2</sub> Ti <sub>1-x</sub> Sn <sub>x</sub> O <sub>3</sub> ( $0 \leq x \leq 0.10$ ) for energy harvester application	72

Table 4.5 The piezoelectric properties for energy harvester of  $\text{Ba}_{0.8}\text{Sr}_{0.2}\text{Ti}_{1-x}\text{Sn}_x\text{O}_3$  ( $0 \leq x \leq 0.10$ ) ceramics at different sintering temperatures

83

©This item is protected by original copyright

## LIST OF FIGURES

		<b>PAGE</b>
Figure 1.1	Roadmap of energy harvesting (Cain & Mitcheson, 2012)	2
Figure 1.2	The piezoelectric effect (Shao, Hao and Wang, Hongxia and Fang, 2019)	3
Figure 2.1	The schematic of a piezoelectric material, showing the polarisation direction and the mechanical stress axis (Moheimani, S.R., Fleming, 2006)	13
Figure 2.2	Cubic prototype perovskite structure	18
Figure 2.3	A perovskite structure can be (a) non-centrosymmetric or (b) centrosymmetric	19
Figure 2.4	The distortion and asymmetric of TiO <sub>6</sub> octahedral in the perovskite structure BaTiO <sub>3</sub> (West et al., 2004)	19
Figure 2.5	Illustration of the hysteresis loop of ferroelectric (B. Jaffe, W. R. Cook, 1971)	20
Figure 2.6	Phase diagram of PZT (Panda & Sahoo, 2015)	21
Figure 2.7	The phase transition temperature at dielectric curve of BaTiO <sub>3</sub> for cubic perovskite structure (Villafuerte-Castrejón et al., 2016)	23
Figure 2.8	(a) XRD pattern of BST ceramics at different ball milling time; (b) XRD pattern of BST ceramics at a different sintering temperature (Mudinepalli et al., 2015)	26
Figure 2.9	Grain size dependence of the piezoelectric constant $d_{33}$ of BST ceramics (Mudinepalli et al., 2015)	26

Figure 2.10	Phase diagram of BSTS based on dielectric measurements (Zaitouni et al., 2020)	33
Figure 3.1	The flow chart of samples preparation process	38
Figure 3.2	The illustration of Bragg's law derivation (West, 2014)	40
Figure 3.3	Block diagram of impedance spectroscopy	42
Figure 3.4	Scanning electron microscope (SEM) for microstructure analysis	43
Figure 3.5	The illustration of poling process	44
Figure 3.6	Piezoelectric measurement setup	44
Figure 4.1	The XRD patterns of $\text{Ba}_{0.8}\text{Sr}_{0.2}\text{TiO}_3$ powder at $2\theta$ from $15^\circ$ to $80^\circ$	46
Figure 4.2	The enlarge XRD patterns in $2\theta$ range from $44.8^\circ$ to $46.0^\circ$ for $\text{Ba}_{0.8}\text{Sr}_{0.2}\text{TiO}_3$	47
Figure 4.3	(a) XRD patterns of $\text{Ba}_{0.8}\text{Sr}_{0.2}\text{Ti}_{1-x}\text{Sn}_x\text{O}_3$ ( $0 \leq x \leq 0.10$ ) powder at $2\theta = 15^\circ$ to $80^\circ$ , (b) the enlarge XRD patterns in $2\theta$ range from $44.5^\circ$ to $46.5^\circ$	49
Figure 4.4	The lattice parameter of $\text{Ba}_{0.8}\text{Sr}_{0.2}\text{Ti}_{1-x}\text{Sn}_x\text{O}_3$ ( $0 \leq x \leq 0.10$ )	51
Figure 4.5	The unit cell volume of $\text{Ba}_{0.8}\text{Sr}_{0.2}\text{Ti}_{1-x}\text{Sn}_x\text{O}_3$ ( $0 \leq x \leq 0.10$ )	51
Figure 4.6	The temperature dependence of dielectric constant for $\text{Ba}_{0.8}\text{Sr}_{0.2}\text{TiO}_3$	53
Figure 4.7	The capacitance versus frequency for $\text{Ba}_{0.8}\text{Sr}_{0.2}\text{TiO}_3$	54
Figure 4.8	The conductivity versus frequency for $\text{Ba}_{0.8}\text{Sr}_{0.2}\text{TiO}_3$	55
Figure 4.9	The conductivities of various classes of materials (Moulson & Herbert, 2003)	55

Figure 4.10	The dielectric loss versus frequency for $\text{Ba}_{0.8}\text{Sr}_{0.2}\text{TiO}_3$ at temperature from $-5\text{ }^\circ\text{C}$ to $140\text{ }^\circ\text{C}$	56
Figure 4.11	The dielectric constant versus temperature measure at 1 kHz	59
Figure 4.12	The inverse dielectric constant of $\text{Ba}_{0.8}\text{Sr}_{0.2}\text{Ti}_{1-x}\text{Sn}_x\text{O}_3$ as a function of temperature	62
Figure 4.13	The $\ln(1/\varepsilon_r - 1/\varepsilon_m)$ versus $\ln(T-T_m)$ for $\text{Ba}_{0.8}\text{Sr}_{0.2}\text{Ti}_{1-x}\text{Sn}_x\text{O}_3$ ( $0 \leq x \leq 0.10$ ) at 1 kHz	63
Figure 4.14	The capacitance versus frequency for $\text{Ba}_{0.8}\text{Sr}_{0.2}\text{Ti}_{1-x}\text{Sn}_x\text{O}_3$ ( $0 \leq x \leq 0.10$ ) at $30\text{ }^\circ\text{C}$	64
Figure 4.15	The conductivity versus frequency for $\text{Ba}_{0.8}\text{Sr}_{0.2}\text{Ti}_{1-x}\text{Sn}_x\text{O}_3$ ( $0 \leq x \leq 0.10$ ) at $30\text{ }^\circ\text{C}$	65
Figure 4.16	The dielectric loss versus temperature for $\text{Ba}_{0.8}\text{Sr}_{0.2}\text{Ti}_{1-x}\text{Sn}_x\text{O}_3$ ( $0 \leq x \leq 0.10$ ) at 1 kHz	66
Figure 4.17	Arrhenius plots of conductivity versus temperature of $\text{Ba}_{0.8}\text{Sr}_{0.2}\text{Ti}_{1-x}\text{Sn}_x\text{O}_3$ ( $0 \leq x \leq 0.10$ ) at $100\text{ }^\circ\text{C}$ to $140\text{ }^\circ\text{C}$	68
Figure 4.18	The SEM images for $\text{Ba}_{0.8}\text{Sr}_{0.2}\text{Ti}_{1-x}\text{Sn}_x\text{O}_3$ ceramics at (a) $x = 0$ , (b) $x = 0.02$ , (c) $x = 0.04$ , (d) $x = 0.06$ , (e) $x = 0.08$ and (f) $x = 0.10$ sintered at $1400\text{ }^\circ\text{C}$	70
Figure 4.19	The comparison of dielectric constant for $\text{Ba}_{0.8}\text{Sr}_{0.2}\text{Ti}_{1-x}\text{Sn}_x\text{O}_3$ ceramics at (a) $x = 0$ , (b) $x = 0.02$ , (c) $x = 0.04$ , (d) $x = 0.06$ , (e) $x = 0.08$ and (f) $x = 0.10$ between sinteres at $1400\text{ }^\circ\text{C}$ and $1450\text{ }^\circ\text{C}$	75
Figure 4.20	The dielectric constant vs. temperature for $\text{Ba}_{0.8}\text{Sr}_{0.2}\text{Ti}_{1-x}\text{Sn}_x\text{O}_3$ ( $0 \leq x \leq 0.10$ ) ceramics sintered $1450\text{ }^\circ\text{C}$	78
Figure 4.21	The SEM micrograph for $\text{Ba}_{0.8}\text{Sr}_{0.2}\text{Ti}_{1-x}\text{Sn}_x\text{O}_3$ ceramics at (a) $x = 0$ , (b) $x = 0.02$ , (c) $x = 0.04$ , (d) $x = 0.06$ , (e) $x = 0.08$	

and (f)  $x = 0.10$  sintered at  $1450\text{ }^{\circ}\text{C}$  with its histogram of grain size distribution

80

©This item is protected by original copyright

## LIST OF ABBREVIATIONS

BaTiO <sub>3</sub>	Barium Titanate
BST	Barium Strontium Titanate
BSTS	Barium Strontium Titanate Stannate
EDX	Energy Dispersive X-ray
MPB	Morphotropic Phase Boundary
PZT	Lead Zirconate Titanate
SEM	Scanning Electron Microscopy
XRD	X-ray Diffraction
MLCC	Multi Layered Ceramics Capacitors
BaCO <sub>3</sub>	Barium Carbonate
SrCO <sub>3</sub>	Strontium Carbonate
TiO <sub>2</sub>	Titanium Oxide
SnO <sub>2</sub>	Stannum Oxide
BPT	Barium Lead Titanate
PbNb <sub>2</sub> O <sub>6</sub>	Lead Meta Niobate
PT	Lead Titanate
BNT	Bismuth Sodium Titanate
BiTiO <sub>3</sub>	Bismuth Titanate
RoHS	Restriction of Hazardous Substances
Pt	Platinum
SiC	Silicon carbide
DC	Direct current
ICDD	Inorganic Crystallography Diffraction Database
PDF	Powder Diffraction Files
FOM	Figures of merits

## LIST OF SYMBOLS

$d_{33}$	Piezoelectric constant
$g_{33}$	Piezoelectric voltage constant
$f$	Frequency
$A$	Electrode area
$C$	Capacitance
$d$	Interplanar spacing
$R$	Resistance
$S$	Strain
$T_c$	Curie Temperature
$t$	Tolerance factor
$\epsilon_0$	Dielectric constant in vacuum
$\epsilon_r$	Relative dielectric constant
$\sigma$	conductivity
$\theta$	Diffraction angle
$\lambda$	Wavelength of X-rays
$\rho$	Resistivity
$\omega$	Angular frequency
$\tan \delta$	Dielectric loss
$D$	Charge displacement
$T$	applied stress
$T_{cw}$	Curie-Weiss constant
$\Delta T$	Deviation from the Curie-Weiss law
$r_A$	Ionic radii of A-site cation
$r_B$	Ionic radii of B-site cation
$r_O$	Ionic radii of oxygen anion
$E_a$	Activation energy
eV	Electron volt
F	Farad
°C	Degree celcius
P	Power output
Q	Charge
$Z'$	Impedance
$l$	Thickness of the sample

# Sifat Dielektrik dan Piezoelektrik yang Dipertingkatkan $Ba_{0.8}Sr_{0.2}Ti_{1-x}Sn_xO_3$ untuk Aplikasi Penuaian Tenaga

## ABSTRAK

Piezoelektrik telah membantu meningkatkan kehidupan seharian kita dengan menghasilkan banyak aplikasi berguna seperti suntikan bahan api automotif, akselerometer, transformer dan motor piezoelektrik, kawalan getaran, sistem penentududukan mikro, pengesan ultrabunyi, penjana, pencetak inkjet, dan penuai tenaga. Penuai tenaga digunakan untuk menukar daya menjadi tenaga elektrik. Bahan piezoelektrik mendapat perhatian paling banyak berbanding kaedah lain kerana bahan itu sendiri secara langsung dapat menukar tenaga regangan yang diterapkan menjadi tenaga elektrik. Walau bagaimanapun, bahan piezoelektrik yang paling praktikal yang terdapat di pasaran ialah Plumbum Zirkonat Titanat (PZT) yang mengandungi sejumlah besar Plumbum (Pb) yang memberi implikasi buruk kepada alam sekitar. Keadaan ini memaksa penemuan bahan piezoelektrik bebas plumbum dalam beberapa tahun ini. Seramik berasaskan Barium Titanat ( $BaTiO_3$ ) telah menjadi calon yang menjanjikan sifat yang mungkin setanding dengan Pb apabila didopkan dengan unsur lain. Dalam kajian ini,  $Ba_{0.8}Sr_{0.2}Ti_{1-x}Sn_xO_3$  (di mana  $x = 0, 0.02, 0.04, 0.06, 0.08$  dan  $0.10$  telah disediakan melalui kaedah tindak balas keadaan pepejal konvensional. Sampel dicirikan menggunakan Pembelauan Sinar-X (XRD), Penganalisis Spektroskopi Impedansi, Penganalisis Uji Piezoelektrik dan Mikroskopi Elektron Pengimbasan (SEM). Analisis XRD menunjukkan,  $Ba_{0.8}Sr_{0.2}Ti_{1-x}Sn_xO_3$  mempunyai peralihan fasa struktur dari tetragonal ke kubik apabila kandungan Sn meningkat. Analisis dielektrik,  $Ba_{0.8}Sr_{0.2}Ti_{1-x}Sn_xO_3$  menunjukkan suhu Curie,  $T_c$  beralih ke arah suhu yang lebih rendah dari  $65^\circ C$  hingga  $5^\circ C$  disebabkan oleh penggantian  $Sn^{4+}$  dengan radius ion yang lebih besar daripada  $Ti^{4+}$  di bahagian B. Komposisi pada  $x = 0$  mempunyai pemalar dielektrik tertinggi disebabkan oleh momen dipol spontan yang banyak. Walau bagaimanapun, penggantian Sn dengan  $x = 0.02$  menunjukkan sedikit penurunan pada pemalar dielektrik. Bagi sampel dengan  $x = 0.04$ , pemalar dielektrik telah menunjukkan terdapat dua peralihan fasa pada  $40^\circ C$  (fasa tetragonal - kubik) dan fasa lain yang berdekatan dengan  $\sim 25^\circ C$  yang merupakan fasa ortorhombik - teragonal ( $T_{O-T}$ ). Kewujudan fasa orthorhombik - teragonal ( $T_{O-T}$ ) telah meningkatkan pemalar dielektrik. Pada  $x = 0.06$  dan  $0.08$ , menunjukkan penurunan berterusan dielektrik dengan peningkatan kandungan Sn disebabkan oleh perubahan struktur kepada struktur kubik. Walau bagaimanapun, pemalar dielektrik sampel dengan  $x = 0.10$  meningkat secara drastik kerana kesan mencubit di mana fasa rhombohedral - orthorhombik ( $T_{R-O}$ ) dan fasa orthorhombic - tetragonal ( $T_{O-T}$ ) bergabung, membentuk satu puncak yang luas di  $T_c$ . Pengukuran piezoelektrik menunjukkan sampel dengan struktur tetragonal,  $x = 0$ , mempunyai nilai  $d_{33}$  yang tinggi sebanyak  $95 \text{ pC/N}$ , nilai  $g_{33}$  sebanyak  $8.66 \times 10^{-3} \text{ Vm/N}$  dan mempunyai kuasa keluaran,  $P$  yang tinggi sebanyak  $0.8227 \text{ pm}^3/\text{J}$  pada suhu bilik, yang sesuai untuk aplikasi penuai tenaga piezoelektrik. Apabila, Sn didopkan dengan  $Ba_{0.8}Sr_{0.2}TiO_3$ , nilai tertinggi bagi pemalar piezoelektrik  $d_{33}$  adalah sebanyak  $61 \text{ pC/N}$ , nilai  $g_{33}$  sebanyak  $3.77 \times 10^{-3} \text{ Vm/N}$  dan mempunyai kuasa keluaran,  $P$  yang tinggi sebanyak  $0.2300 \text{ pm}^3/\text{J}$  direkodkan pada  $x = 0.02$ .

# Enhanced Dielectric and Piezoelectric Properties of $\text{Ba}_{0.8}\text{Sr}_{0.2}\text{Ti}_{1-x}\text{Sn}_x\text{O}_3$ for Energy Harvester Application

## ABSTRACT

Piezoelectricity improved our daily life by producing many useful applications such as automotive fuel injection, accelerometers, piezoelectric transformers and motors, vibration control, micro-positioning systems, ultrasonic sensor, generators, inkjet printers, and energy harvester. The energy harvester is used to convert force into electrical energy. Piezoelectric material becomes the most attention than other material because the material itself can directly convert applied strain energy into electrical energy. However, the most practical piezoelectric material available in the market is Lead Zirconate Titanate (PZT) which contained a large amount of Lead (Pb) that gives severe implications to the environment. This situation has forced the finding of lead-free piezoelectric material in recent years. Barium Titanate ( $\text{BaTiO}_3$ )-based ceramic has become the promising candidate that could have comparable properties to Pb when doped with other elements. In this study,  $\text{Ba}_{0.8}\text{Sr}_{0.2}\text{Ti}_{1-x}\text{Sn}_x\text{O}_3$  where  $x = 0, 0.02, 0.04, 0.06, 0.08$  and  $0.10$  were prepared using conventional solid-state reaction method. The samples were characterised using X-ray Diffraction (XRD), Impedance Spectroscopy analyser, Piezoelectric Test analyser, and Scanning Electron Microscopy (SEM). The XRD analysis shows that  $\text{Ba}_{0.8}\text{Sr}_{0.2}\text{Ti}_{1-x}\text{Sn}_x\text{O}_3$  had a structural phase transition from tetragonal to cubic when Sn content increased. The dielectric analysis of,  $\text{Ba}_{0.8}\text{Sr}_{0.2}\text{Ti}_{1-x}\text{Sn}_x\text{O}_3$  shows the Curie temperature,  $T_c$  shifted towards lower temperature from  $65^\circ\text{C}$  to  $5^\circ\text{C}$  was due to the replacement of  $\text{Sn}^{4+}$  with larger ionic radii than  $\text{Ti}^{4+}$  at B-sites. The composition with  $x = 0$  has the highest dielectric constant because of large spontaneous dipole moments. However, the substitution of Sn with  $x = 0.02$  shows a bit decrease in dielectric constant. For  $x = 0.04$ , the dielectric constant has revealed two-phase transition at  $40^\circ\text{C}$  (tetragonal – cubic phases) and another phase near  $\sim 25^\circ\text{C}$ , which belongs to orthorhombic – tetragonal phases ( $T_{O-T}$ ). The existence of orthorhombic – tetragonal phases ( $T_{O-T}$ ) has increased the dielectric constant. At  $x = 0.06$  and  $0.08$ , the dielectric constant decreases by increasing the Sn contents due to the structural changes to the cubic structure. However, the dielectric constant of the sample with  $x = 0.10$  drastically increased due to the pinching effect where rhombohedral – orthorhombic ( $T_{R-O}$ ) phases and orthorhombic – tetragonal ( $T_{O-T}$ ) phases merged, forming one broad peak at  $T_c$ . The piezoelectric measurement shows that a sample with a tetragonal structure,  $x = 0$ , has a high  $d_{33}$  value about  $95\text{ pC/N}$ ,  $g_{33}$  value about  $8.66 \times 10^{-3}\text{ Vm/N}$  has the high output power,  $P$  about  $0.8227\text{ pm}^3/\text{J}$  at room temperature, which is good for piezoelectric energy harvester application. When, Sn is doped in  $\text{Ba}_{0.8}\text{Sr}_{0.2}\text{TiO}_3$ , the highest value of the piezoelectric constant  $d_{33}$  is  $61\text{ pC/N}$ , the value of  $g_{33}$  is  $3.77 \times 10^{-3}\text{ Vm/N}$  and has a high output power,  $P$  of  $0.2300\text{ pm}^3/\text{J}$  is recorded at  $x = 0.02$ .

## CHAPTER 1 : INTRODUCTION

### 1.1 Research Background

Piezoelectric ceramic material is known to exhibit a unique effect called direct effect and converse effect. The direct effect is the capability of the material to change mechanical stress into electrical charge. In contrast, the converse effect is the ability of the material to produce mechanical force when an electric current is applied. These dual effects enable piezoelectric material to be used in various applications such as automotive fuel injection, accelerometers, piezoelectric transformers and motors, vibration control, micro-positioning systems, ultrasonic sensors and generators, inkjet printers, and energy harvester. Recently, the piezoelectric energy harvester has turn out to be the best energy harvester transducer options in the electronic industry. The usage of piezoelectric material for energy harvester has been utilized by California state for piezoelectric energy harvester application, where piezoelectric ceramics are scattered half-mile of highway in aiming to power 5000 homes in future (California Piezoelectric Highway, 2017). In order to understand the piezoelectric, the figure of merits for piezoelectric parameters such as the piezoelectric pressure coefficient ( $d_{ij}$ ), the piezoelectric voltage constant ( $g_{ij}$ ), power (P), and its temperature dependences is crucial to be understood.

The researchers have investigated several research areas to enhance the performance of energy harvester applications. Cain and Mitcheson have carried out some related project work about energy harvester application. Their work is associated with the energy roadmap, as demonstrated in Figure 1.1(Cain & Mitcheson, 2012). Based on Figure 1.1, each research area has its targets, assurance of deliverables, technologies, and enabling in science that was predicted to be achieved by a particular year. From 2014

until mid-2015, work on an intelligent adaptive system was performed and followed with nanoscale devices until mid-2016. After that, the enhancement of energy harvester application continued in the development of hybrid devices. However, as 2018 progresses and several years ahead, the most exciting research field for researchers will be device integration and the production of new materials. As a result, the aim of this research is to discover and develop new piezoelectric materials for energy harvester applications.

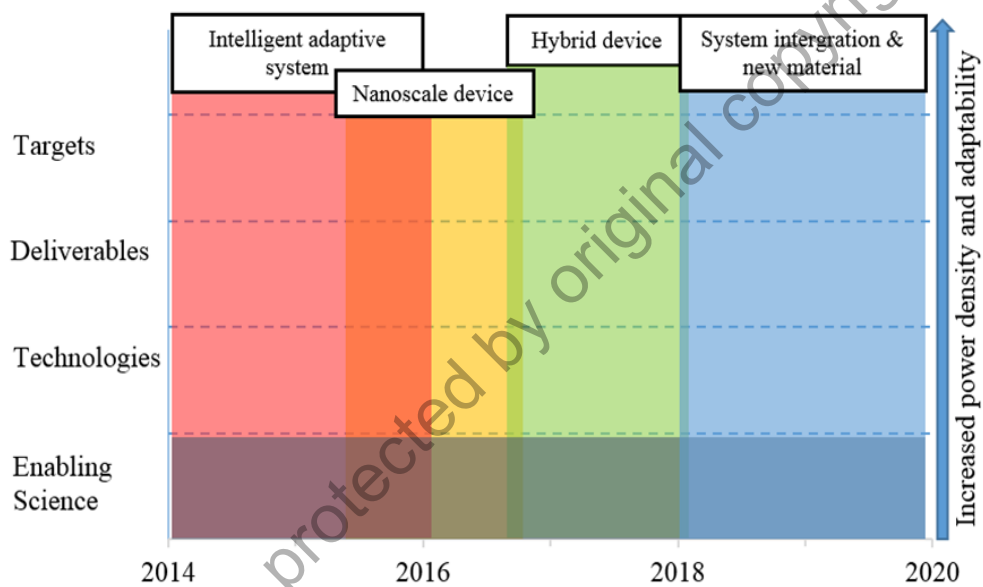


Figure 1.1 Roadmap of energy harvesting (Cain & Mitcheson, 2012)

## 1.2 Mechanism of piezoelectric materials

Piezoelectric material is classified by the dielectric materials that belongs in the class of non-centrosymmetric crystals structure. Even though the piezoelectric crystal is not symmetrically arranged but their electrical charges are perfectly balanced due to piezoelectric materials having random direction of dipoles in unit cells. However, the electric dipoles in the crystal become oriented during the polarisation process. This

process helps the direct piezoelectric effect happen where the electrical energy was generated when the mechanical stress is applied. Therefore, the oriented electric dipoles creates positive and negative charges on opposite sides, resulting in an electric field across the crystal (Vijaya, 2017).

In another way, when the external electric field is applied to the materials, symmetric displacements of anions and cations occur, resulting in significant net crystal deformation. The resultant strain is directly proportional to the applied electric field. The strain in a piezoelectric material is expansive or compressive, depending on the polarity of the applied field. This effect is known as the converse or indirect piezoelectric effect. Figure 1.2 shows the type of piezoelectric effect (Vijaya, 2017).

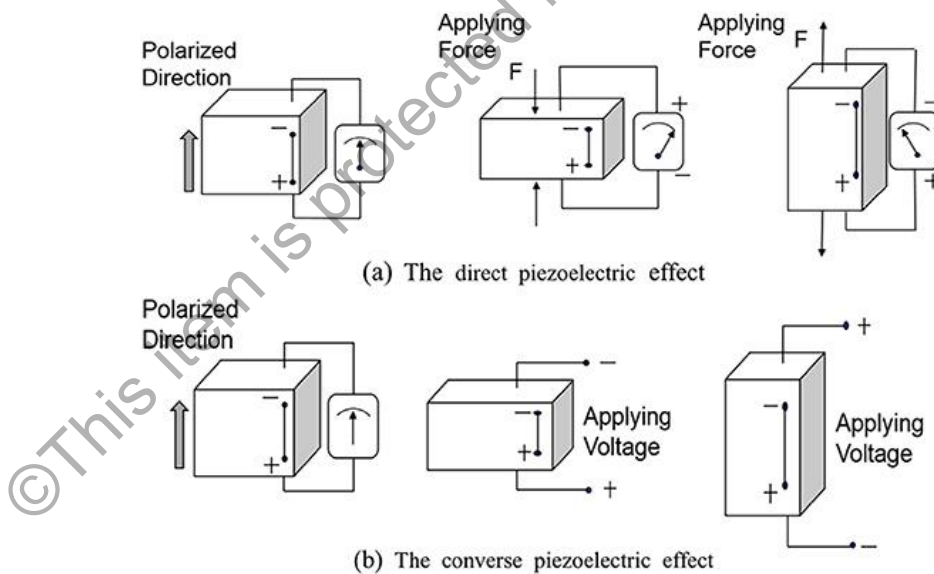


Figure 1.2 The piezoelectric effect (Shao, Hao and Wang, Hongxia and Fang, 2019)

### 1.3 Problem statement

To date, the most used material for the piezoelectric application is Lead Zirconate Titanate (PZT). It is because PZT exhibit high piezoelectric constant (375 pC/N) and high mechanical coupling coefficient, exhibit high curie temperature ( $T_c$ ) in the range of 300 to 400 °C, can be easily poled, has a wide range of dielectric constant, relatively easy to sinter at lower temperatures, and form solid solution compositions with variety of constituents, thus enabling a wide range of available properties (Bobic et al., 2018). Presently PZT-based piezoelectric ceramics are leading materials for piezoelectric transducers because of their impressive piezoelectric properties. However, more recently, there is now an increase in concern about the toxicity of lead-containing devices from the restriction of hazardous substances directive regulations (Leontsev & Eitel, 2010). Therefore, in 2015, the used of lead in electronic devices was completely restricted by The RoHS (Fasquelle et al., 2015)(Zheng et al., 2018). In order to resolve this problem, future research will be focused on the replacement of Pb-based material. Therefore, lead-free perovskite materials have widely investigated recently.

Barium titanate-based material is a promising candidate for lead-free piezoelectric material in piezoelectric material research with nearly PZT characteristics. Barium Titanate has piqued people's attention for more than 60 years because of its appealing properties such as chemically and mechanically very stable, it has ferroelectric properties at room temperature and above and also it is simple to make and use in the form of polycrystalline ceramics (Vijatović et al., 2008a). Because of its high dielectric constant and low loss characterisation, barium titanate ( $\text{BaTiO}_3$ ) is used in capacitors and multilayer capacitors (MLCs) (Vijatović et al., 2008b). However, the piezoelectric constant for  $\text{BaTiO}_3$  is about 191 pC/N, which is lower than PZT. Since then, further

investigations on the enhancement of pure BaTiO<sub>3</sub> by doping with other materials like strontium (Sr) and stannum (Sn) have been among the most intriguing for investigators from time to time.

#### 1.4 Objectives

1. To synthesis the barium strontium titanate stannate (BSTS) with formula Ba<sub>0.8</sub>Sr<sub>0.2</sub>Ti<sub>1-x</sub>Sn<sub>x</sub>O<sub>3</sub> ( $0 \leq x \leq 0.10$ ) by using conventional solid-state reaction method.
2. To determine the dielectric and piezoelectric properties of Ba<sub>0.8</sub>Sr<sub>0.2</sub>Ti<sub>1-x</sub>Sn<sub>x</sub>O<sub>3</sub> ( $0 \leq x \leq 0.10$ ).
3. To correlate between microstructure, electrical and piezoelectric properties of Ba<sub>0.8</sub>Sr<sub>0.2</sub>Ti<sub>1-x</sub>Sn<sub>x</sub>O<sub>3</sub> ( $0 \leq x \leq 0.10$ ).

#### 1.5 Scope of study

The scope of this research is to study the BaTiO<sub>3</sub> based energy harvester material for the replacement of PZT. The research will focus on Sn doped barium strontium titanate (BST) with formula Ba<sub>0.8</sub>Sr<sub>0.2</sub>Ti<sub>1-x</sub>Sn<sub>x</sub>O<sub>3</sub> for  $x = 0, 0.02, 0.04, 0.06, 0.08$  and  $0.10$ . The sample will be prepared using the conventional solid-state reaction method. Then, X-ray Diffraction is used to get the phase purity of Sn doped BST. Instead, all the samples will be characterised to correlate between electrical properties, piezoelectric properties, and surface morphology by varying sintering temperature at 1400 °C and 1450 °C. The

effect of small doping on BST can therefore be concluded whether it can enhance its piezoelectric and dielectric properties.

## **1.6 Thesis structure**

This thesis is arranged with several chapters starting with chapter 1, which includes a brief overview of piezoelectric mechanism, current problem statement regarding piezoelectric material for energy harvester and objectives of this research. Chapter 2 is the literature review related to this research. Several subtopics have been discussed, which is the piezoelectric materials are compared with their respective electrical and piezoelectric properties. In chapter 3 explain the methodology used to synthesise the sample and presented it through a flow chart. Chapter 4 represent the result obtained from this research, including structural analysis, impedance spectroscopy analysis, surface morphology analysis and piezoelectric analysis. Lastly, a summary and the future implementation for this project are presented in Chapter 5

## CHAPTER 2 : LITERATURE REVIEW

### 2.1 Introduction

This chapter describes the detailed literature related to piezoelectric, including its material, the applications, and the current issue. Numerous research for enhancing the electrical and piezoelectric properties of lead-free material was previously reported in the literature. The piezoelectric effect has helped to improve our technology by producing various applications like sonar, energy harvester, and actuator. However, several issues have taken back the advantage of it. Most commercial piezoelectric material is made up of a large amount of lead (Pb). This large amount of Pb used in our daily life can be harmful to human and the environment. Pb is one of the materials that creates hazard while processing that potentially becomes toxic to the environment. Thus, the lead-free piezoelectric material is interesting for researchers to have a material with comparable properties with lead.

### 2.2 Piezoelectricity

Piezoelectricity comes from the Greek word “piezen”, meaning to press or squeeze. The piezoelectric effect was found in 1880 by Jacques and Pierre Curie. They found that some materials like quartz, topaz, and zinblend can generate electrical energy when mechanical force is applied, or these phenomena call the direct piezoelectric effect. The contrast of it is called a converse piezoelectric effect where the mechanical force is produced when an electric current is applied that was mathematically deduced from fundamental thermodynamic principles by Gabriel Lippmann and been confirmed by Curie brothers soon after that (B. Jaffe, W. R. Cook, 1971).

According to B. Jaffe, W. R. Cook, H. Jaffe, there is three significant sources to discover the high piezoelectric effect in ceramic material. First is the discovery of high permittivity or also known as dielectric constant. Second, the discovery of a high dielectric constant is due to ferroelectricity. Ferroelectricity was first discovered in Rochelle salt in 1921 after piezoelectricity was found. It followed with the first ferroelectricity born in ceramic materials ( $\text{BaTiO}_3$ ) in the 1940s (Haertling, 1999). Thus, it is ushering in a new class of ferroelectric with the  $\text{ABO}_3$  perovskite structure.  $\text{BaTiO}_3$  at that time produced a high dielectric constant ( $\epsilon_r = 1200$  at room temperature) and used in capacitor technology up until now. The third was discovering the poling method in which the high voltage was necessary to reverse electrical moments of the ceramics' spontaneous polarised area.

Presently, many companies have commercialised piezoelectric materials for various uses, as shown in Table 2.1. It was observed that most of the commercial material used in piezoelectric technologies such as lead zirconate titanate (PZT), barium lead titanate (BPT), lead meta niobate ( $\text{PbNb}_2\text{O}_6$ ), lead titanate (PT), bismuth sodium titanate (BNT) and bismuth titanate ( $\text{BiTiO}_3$ ). Lead zirconate titanate (PZT) has the highest piezoelectric constant among the other materials. However, the use of lead has been restricted by Restriction of Hazardous Substances (RoHS) due to high toxicity that can cause harm to the universe

Table 2.1 List of commercial material with dielectric constant, piezoelectric constant, piezoelectric voltage constant, Curie temperature and applications

Company	Material	Dielectric constant, $\epsilon_r$	Piezoelectric constant, $d_{33}$ (pC/N)	Piezoelectric voltage constant, $g_{33}$ (mV/N)	Curie temperature, $T_c$ (°C)	Applications	Reference
APC International Ltd.	Lead zirconate titanate (PZT)	1900	400	24.8	360	High performance transducers for medical imaging applications	(APC Materials / APC Materials / Table, 2021)
	Lead zirconate titanate (PZT)	1450	360	27	345	Microphones and vibration pickups with preamplifier	(Piezoceramic Materials, 2021)
Physik Instrumente (PI) GmbH & Co. KG	Bismuth sodium titanate (BNT)	750	120	15	190	Ultrasonic transducer	
	Barium lead titanate (BPT)	950	120	-11.9	150	Sonar and hydroponic	